Some Observations of Solder Joint Failure under Tensile-Compressive Stress

A paper for consideration for presentation at the
ASME Electronic Packaging Conference,
September 29 - October 2, 1993,
Holiday Inn Arena Hotel, Binghamton, NY USA.

by
J.W. Winslow, Jet Propulsion Laboratory of the
California Institute of Technology, Pasadena, CA

I. DESCRIPTION OF THE PROBLEM

For many decades it has been known that the mechanical strength of solders is subject to failure under environments which contain mechanical stresses. In early electronic systems, such failures were avoided primarily by avoiding the use of solder as a mechanical structural component. The rule was first to make sound wiring connections that did not depend mechanically on solder, and only then to solder them.

With miniaturization resulting from use of modern solid state electronic components and Printed Wiring Boards (PWBs), the old rule of thumb has gone by the board. Careful design of modern electronic systems limits the mechanical stresses exerted on solder joints to values less than their yield points, and these joints have become integral parts of the mechanical structures. This has been especially widespread in circuitry intended for use in spacecraft, where the premium for reduction of mass is especially high.

Unfortunately, while these joints are strong enough when new, they have proved vulnerable to fatigue failures as they age. These fatigue failures have restricted the useful lifetimes of their circuits to values which are undesirably small, especially in the case of long mission spacecraft. This is particularly annoying because details of the fatigue mechanism(s) are poorly understood, resulting in large uncertainties when predicting lifetimes, and requiring correspondingly large safety margins in the design of circuit hardware.

Over recent decades, fatigue mechanisms in solders have attracted the attentions of many researchers. While these mechanisms are not the principal subject of this paper, we note from the literature in the field that many different solders have been studied, and that different solders behave rather differently from one another. For a while it seemed that whatever the result of one life study, another soon would come along to refute it. Consequently, in our studies we have opted for the relatively simple case of a single composition, namely eutectic tin-lead solder, i.e. about three atoms of tin for each atom of lead.

We also note from the literature that solder fatigue failures in general are associated with changes in temperature of the hardware, presumably via stresses and/or strains arising from differential thermal expansion between its various mechanical components. In this respect we note that the invention of the “instant-on” TV set has led to a considerable improvement in reliability, albeit at the cost of higher electric bills, through reducing the number of thermal cycles experienced by the hardware during a service lifetime.

Finally, we note from the literature that the phenomenon of creep plays an important role in solder fatigue, For this reason, we selected a thermal cycling test that allows ample time for creep processes to occur. In this selection, of course, we were influenced also by the fact that the temperatures in many typical spacecraft environments change relatively slowly, i.e. on the order of 90 minutes to 24 hours (or more) per thermal cycle.

II. INVESTIGATIVE APPROACH

In testing hardware, the need to allow adequate time for creep processes to occur during the tests restricts the period of the individual thermal test cycle to values on the order of hours, rather than minutes or seconds. Consequently, test acceleration is found in practice through increasing test parameters other than frequency. In particular, the temperature range (AT) of the thermal cycle, i.e. the difference between the maximum and minimum temperatures of the cycle, often is chosen for the principal accelerating parameter.

The risk in increasing AT much beyond that of the service environment, of course, is that the fatigue mechanism may change as a function of temperature. In such a case, the damage resulting during an accelerated test may differ qualitatively, as well as quantitatively, from that found in service. Consequently the amount of acceleration between test and service environments, and the transfer function between test and service lifetimes, may be difficult or impossible to calculate.

Recently a tentative basis for such a transfer function has been proposed (1). The basis of the proposed extrapolation relationship is the equation

$$L_i/L_T = (\Delta T_T/\Delta T_i)^{2.6} \qquad \text{(eqn 1)},$$

where

L_i is the estimated lifetime of the service solder joints under the i^{th} component of the service environment,

L_T is the lifetime observed for the solder joints in the accelerated test,

ΔT_T is the temperature range ($= T_{max} - T_{min}$) for the accelerated test thermal cycle, and

ΔT_i is the temperature range for the i^{th} component of the service thermal environment.

This equation is a simplified version of the Coffin-Manson equation, where the value of the exponent was determined empirically from data given in previous literature.

The experiment designed for this study was a straight-forward test of this proposed relationship, using identical specimens under several thermal cycling environments, each such environment having its own value of ΔT.

III. EXPERIMENTAL DESIGN

To date, our experimental investigation has subjected identical test articles, each consisting of (a) five stub-mounted 14 lead DIPs, and (b) five gull-wing mounted 14 lead DIPs, on a PWB (see Fig 1), to two different thermal cycles. Tensile-compressive mechanical forces were exerted on the solder joints via a conformal coating material encapsulating the DIPs, filling the entire gap between each DIP ceramic body and its PWB. This configuration provided larger than usual driving forces due to the mismatches between coefficients of thermal expansion (CTEs) of the coating material, the DIP leads, the component body, and the PWB.

Note that these Test Articles were designed especially for this study, and do not represent flight quality hardware.

Iv. EXPERIMENTAL DETAILS

To date, two main thermal cycles have been used. Oven temperatures of these cycles are given in Fig 2. Temperatures of the test articles were found to lag behind oven temperature changes by about 15 minutes.

Both cycles had a T_{max} of 100 “C and a test article dwell time of 15 minutes at that temperature (i.e. an oven dwell time of about 30 minutes). Rising ramp times between T_{min} and T_{max} were identical for the two cycles (approximately 63 minutes). For the first type cycle, T_{min} was -25 “C, for a AT of 125 “C, while for the second type, T_{min} was 37°C, giving a AT of 63 “C. Declining ramp times (approximately 40 minutes) also were equal for the two types of cycles. Test article dwell time at T_{min} for the 125 “C cycle was about 1 minute, while the corresponding dwell time for the 63 “C cycle was about 20 minutes. (For a subset of 125 “C test specimens, the dwell at T_{min} was increased by 105 minutes, with little if any effect seen on the stub-mounted DIPs.)

Failure of each specimen was defined by an electrical continuity loss event detector (2). For each DIP the leads were daisy-chained together through a set of electrical connections involving shorting wires between the lead shoulders, and between solder pad lands on the PWBS. The shoulder leads connected between the shoulders of leads 1 thru 3, 4 and 5, 6 thru 9, 10 and 11, and 12 thru 14. The land wires connected between PWB lands connected to the solder pads of leads 3 and 4, 5 and 6, 9 and 10, and 11 and 12. The solder pads for leads 1 and 14 were connected by PWB lands to bifurcated terminals, which in turn were connected to the corresponding channel of the event detector.

The event detector was set so that any increase of channel resistance to greater than 200 ohms for more than 2 ns would trigger a latching circuit, throwing a flag to indicate loss of electrical continuity in that channel. Flags were polled twelve times per cycle, with all flags reset after each poll. In this test, the basic thermal cycle lasted 171 minutes, so that consecutive polls occurred at 14,25 minute intervals. The number of flags thrown in each channel was counted up during each thermal cycle, with all counters reset to zero at the end of each cycle.

Unfortunately, the event detector proved vulnerable to electrical noise from our ovens, so that false signals were numerous when our test articles were unshielded. With careful attention to shielding of test articles and the cables connecting them to the detector, these false signals were reduced in number to a reasonable level. However, it still was necessary to pay close attention to event indications over several consecutive cycles to identify electrical continuity loss with reasonable certainty.

v. EXPERIMENTAL RESULTS

For stub mounted DIP specimens, the number of cycles to failure was found almost independent of temperature range AT (Fig 3). There was a difference in spread between the two data sets, that for the AT = 125 'C data ranging over a factor of about ten, while the AT = 63 'C set (except for the final specimen) ranged over a factor of about four. However, the ratio of about 6 predicted by the proposed extrapolation relationship between the lifetimes for the two values of AT, was conspicuous by its absence.

For the case of the gull-wing mounted DIPs, the story was quite different (Fig 4). Here the number of cycles to failure for the smaller value of AT was roughly three times that found for the larger AT. The AT = 63 °C data also suggest that for gull-wing mounted DIPs there are two distinctly different populations, (1) those failing at less than 400 thermal cycles, and (2) those lasting longer.

VI. DISCUSSION OF RESULTS

We have noted in the past that solder joints in the gull-wing configuration, when thermal cycled, show surface cracks in the solder that first appear around the heel of the joint. Then, as thermal cycling continues, the cracks propagate along both sides of the lead foot until they reach the toe area. Then, the lead separates from the solder pad, as shown in Fig. 5.

Figures 6 & 7 show scanning electron microscope (SEM) photos of cross sections of two leads (Nos 6 & 9) of one of our gull-wing mounted DIPs, taken some two cycles after failure as defined by our event detector criteria. We note that lead #9 has separated completely from its solder pad, while lead #6 (directly across the DIP from #9) has separated from its pad along most of the length of the foot from the heel toward the toe, but remains attached at the toe.

Based on the above observations, we speculate that the two DIP configurations fail by different mechanisms. To us it appears that the stub-mounted DIPs fail primarily by simple tensile failure of the solder, while failure of the gull-wing configuration is dominated by crack propagation through the solder, parallel to the foot.

We note that according to existing literature [3], [4] near-eutectic solder fails under thermal cycling by a three step mechanism. First, the grain size of the two-phase system coarsens, the alpha phase, lead-rich inclusions growing larger and farther apart within the tin-rich, beta phase matrix. Then, micro-cracks appear, primarily in the beta phase regions. Finally, the cracks grow until they join each other, and a complete macroscopic separation occurs. During all three steps, segregation of lead from tin atoms continues, until the respective phases become nearly pure lead and tin,

We speculate from the observations reported above, that in the stub mounted configuration the tensile strength of our solder fails with relatively little crack propagation. If the first two steps were to occur significantly at only T_{max}, this could well account for the observation that our choices of the two values of ΔT on the stub mounted case had minimal effect on lifetime.

Conversely, in the gull-wing configuration the crack propagation step appears to play a relatively large role in the fracture process. This would be consistent with the speculation that the crack propagation process occurs at T_{min} as well as T_{max}, and consequently, the observed number of cycles to failure is sensitive to the values chosen for ΔT.

If the above speculations can be verified by further work, it would be interesting to construct a computer model using various solder joint configurations to evaluate quantitatively the various steps of the joint degradation mechanism.

With respect to the original goal of our experiments, it appears that the degradation process of this material is more complex than contemplated by the proposed extrapolation relationship. This severely limits the applicability of that relationship, and suggests that further effort to explore the role of joint geometry will be required.

At this time, we have no speculations with respect to the apparent hi-modal distribution of the AT=63°C data. Suggestions from the audience will be welcomed.

REFERENCES

1. JPL Publication 89-35, "Magellan/Gallileo Solder Joint Failure Analysis & Recommendations", by Ronald G. Ross Jr, dated September 15, 1989.

2. Event Detector, Analysis and Technology, Inc. Model No. 128

3. Frear, D.R. 1987 "Microstructural Observations of the Sn-Pb Solder/Cu System and Thermal Fatigue of the Solder Joint", PhD Thesis U Calif, Berkeley, Ca.

4. Frankland, H. G., Sanderson, I., Sawyer, N. J., & Crownhart,C. 1969,"Final Report for LM Landing Radar, Solder Joint Research Program,Improving the Reliability of Stud Type Solder Joints" Ryan Aeronautical Company Report No. 53969-55, dated 15 April 1969,

This research was performed at the Jet Propulsion Laboratory of the California Institute of Technology, Pasadena CA, under a contract with the National Aeronautics and Space Administration.

FIGURE CAPTIONS

FIG 1, Test Article 24A.

FIG 2. Thermal Cycles.

FIG 3, Failures for Stub-mounted DIPs.

FIG 4. Failures for Gullwing-mounted DIPs,

FIG 5. SEM Photos - DIP leads at about 205 thermal cycles after first pin failure.

FIG 6. SEM Photos of x-sectioned lead #9, specimen TA24D-2; S/N 144, at about 2 cycles after failure. Photos after cycle #377; failure at cycle #375.

FIG 7. SEM Photos of x-sectioned lead #6, DIP S/N 144, about 2 cycles after DIP failure. Photos after cycle #377; failure at cycle #375.

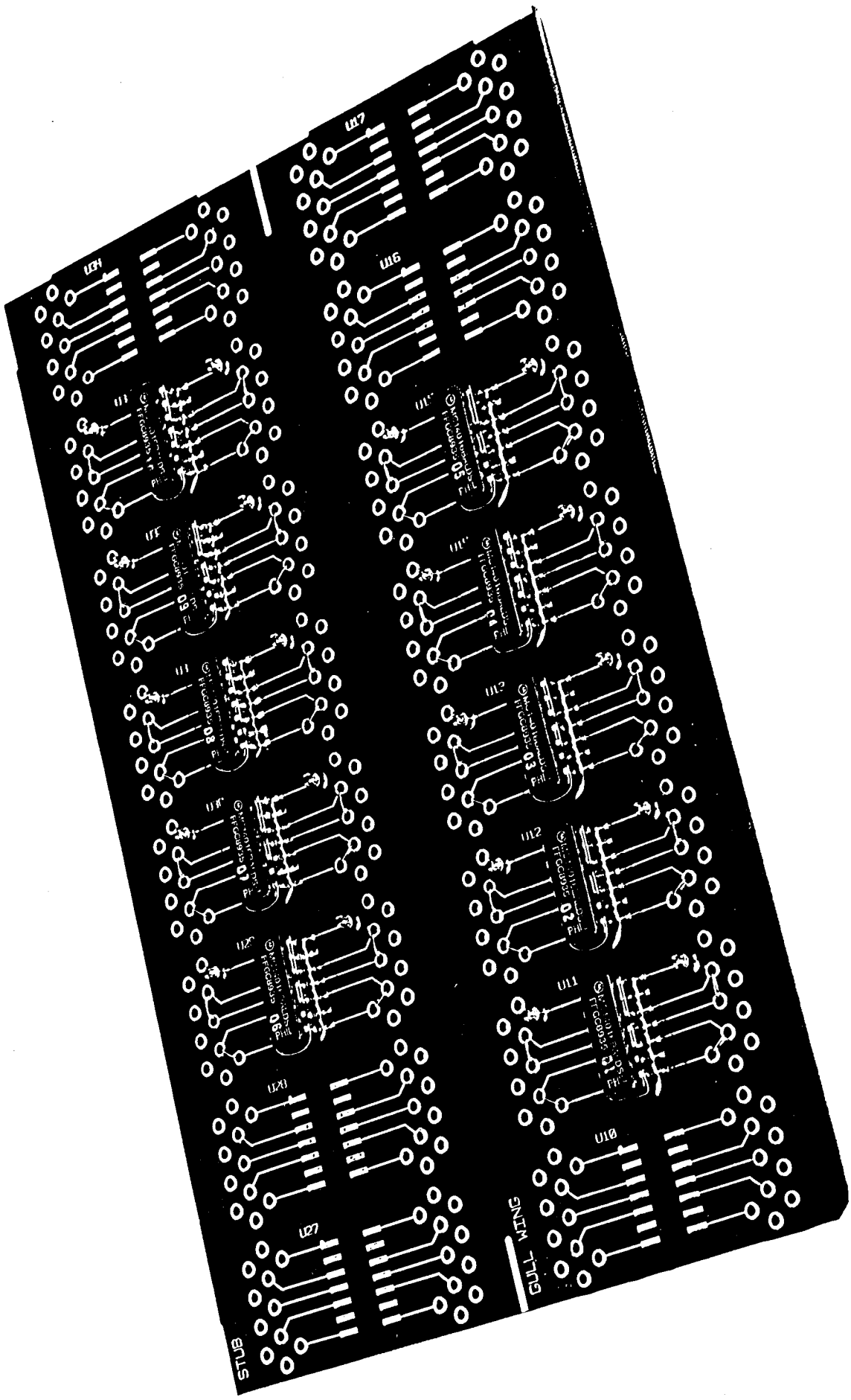
U17
U16
U15
U14
U13
U12
U11
U10
U27
U26
U25
U24
U23
U22
U21
U20
SLOT
GULL WING

FIG 1. TA 24A

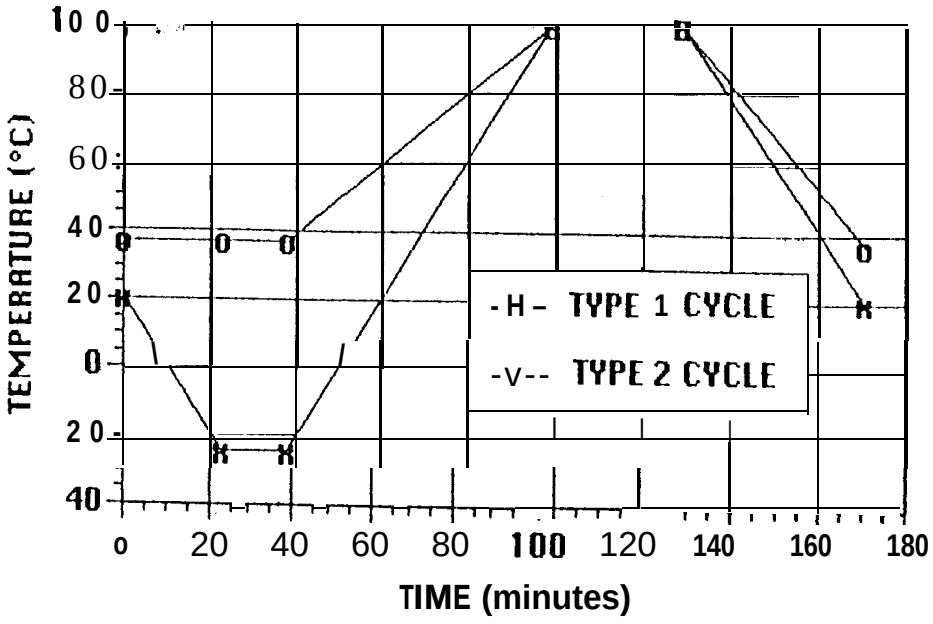

FIG 2. Thermal Cycles

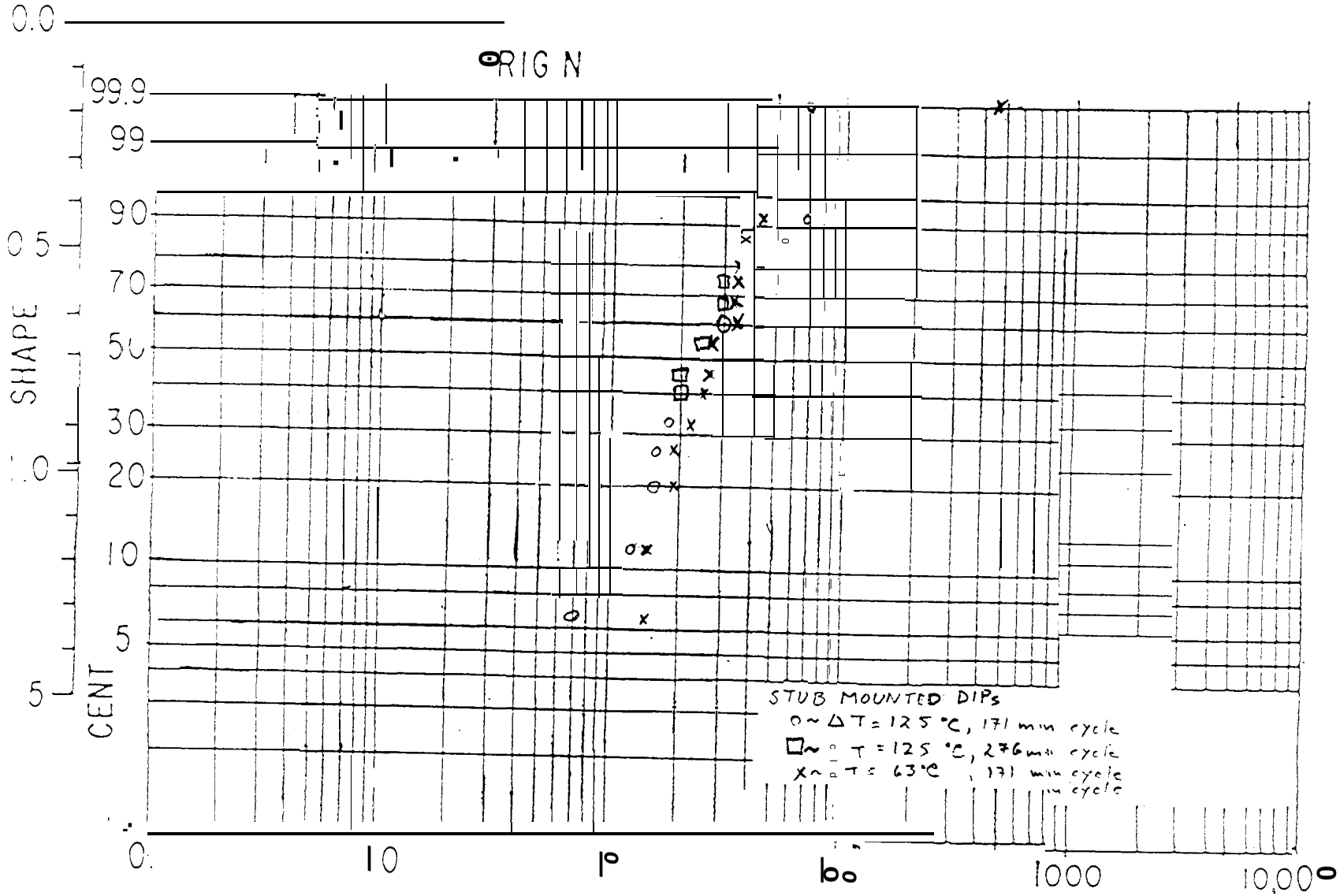

Fig 3 Failures for stub-mounted DIPs

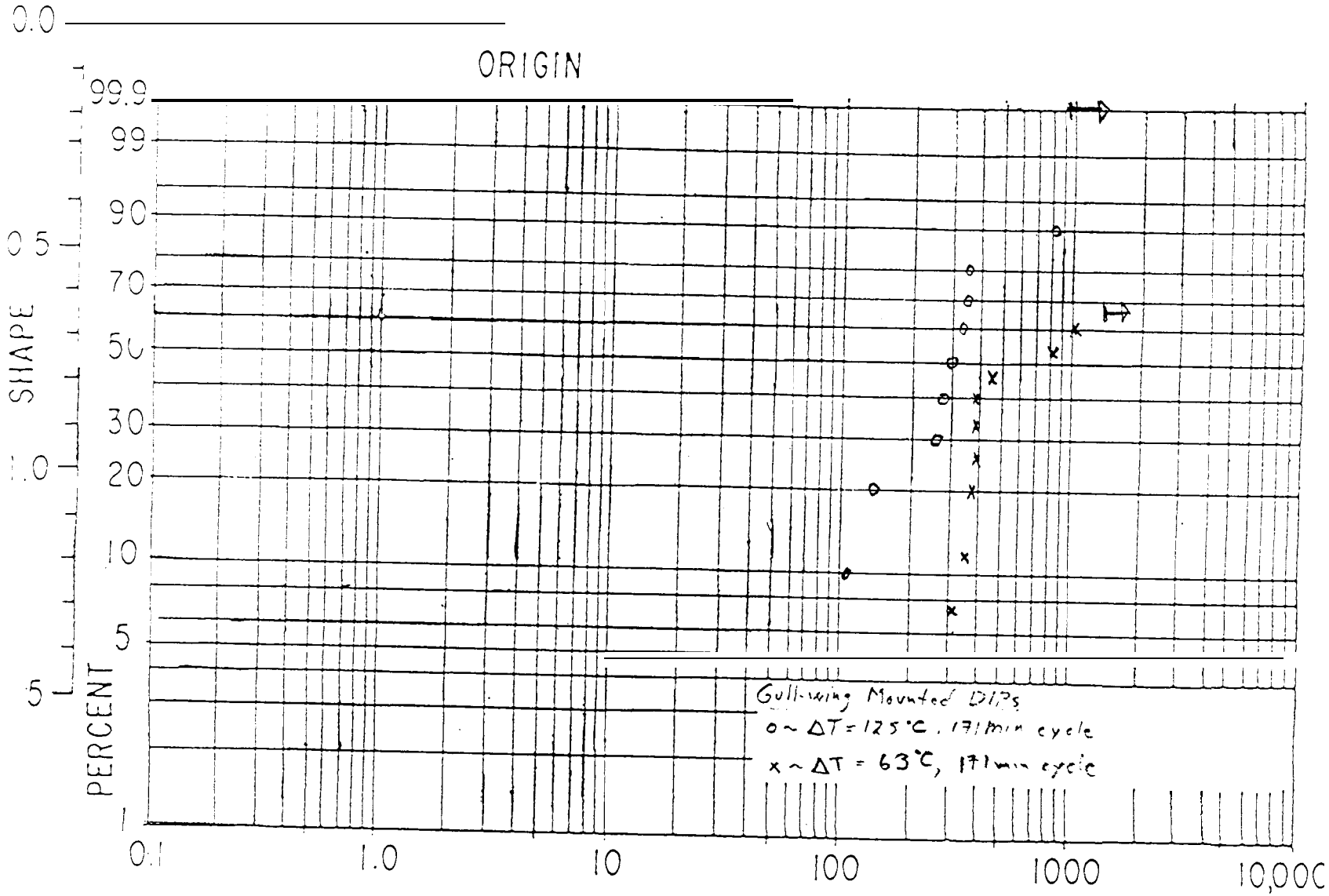

Fig 4 Failures for Gull wing Mounted DIPs

FIG 5

SEM Photos - DIP leads at about 205 thermal cycles after first pin failure.

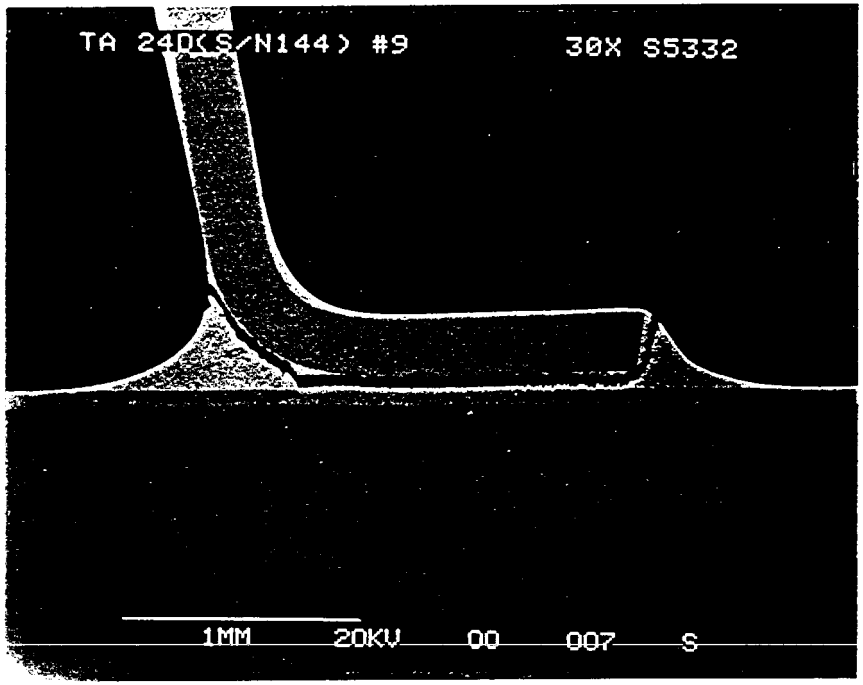

FIG 6

SEM Photos of x-sectioned lead #9, specimen TA24D-2, S/N 144, at about 2 cycles after failure. Photos after cycle #377, failure at cycle #375.

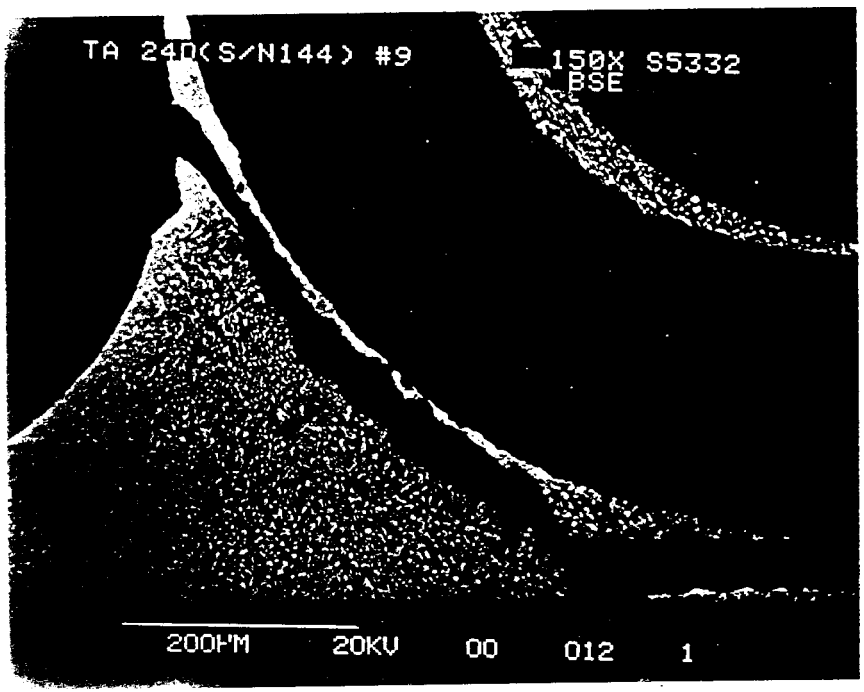

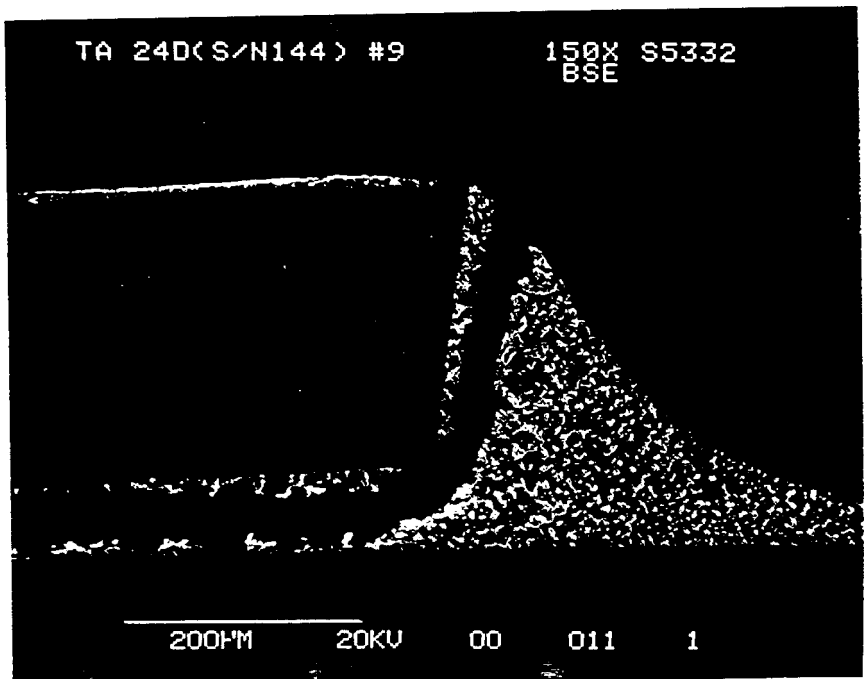

FIG 7

SEM Photos of x-sectioned lead #6, DIP S/N 144, about 2 cycles after DIP failure. Photos after cycle #377; failure at cycle #375.